International Journal of Biological Macromolecules 126 (2019) 1167–1176

Contents lists available at ScienceDirect

International Journal of Biological Macromolecules

journal homepage: http://www.elsevier.com/locate/ijbiomac

Structural and enzymatic characterization of Peruvianin-I, the first germin-like protein with proteolytic activity

Wallace T. da Cruz [a], Eduardo H.S. Bezerra [a], Thalles B. Grangeiro [b], Jose L.S. Lopes [c], Maria Z.R. Silva [a], Márcio V. Ramos [a], Bruno A.M. Rocha [a], Jefferson S. Oliveira [d], Deborah C. Freitas [a], Cleverson D.T. Freitas [a,*]

[a] Departamento de Bioquímica e Biologia Molecular, Universidade Federal do Ceará, Campus do Pici, CEP 60440-554, Fortaleza, Ceará, Brazil
[b] Departamento de Biologia, Universidade Federal de Ceará, Fortaleza, Brazil
[c] Instituto de Física, Universidade de São Paulo, CEP 05508-090 São Paulo, SP, Brazil
[d] Universidade Federal do Piauí, Campus Ministro Reis Velloso, Departamento de Biomedicina, Parnaíba, Piauí, Brazil

ARTICLE INFO

Article history:
Received 16 November 2018
Received in revised form 4 January 2019
Accepted 5 January 2019
Available online 6 January 2019

Keywords:
GLP
Laticifer
Oxalate oxidase

ABSTRACT

The germin-like protein (GLP) purified from *Thevetia peruviana*, Peruvianin-I, is the only one described as having proteolytic activity. Therefore, the goal of this study was to investigate the structural features responsible for its enzymatic activity. Although the amino acid sequence of Peruvianin-I showed high identity with other GLPs, it exhibited punctual mutations, which were responsible for the absence of oxalate oxidase activity. The phylogenetic analysis showed that Peruvianin-I does not belong to any classification of GLP subfamilies. Moreover, Peruvianin-I contains a catalytic triad found in all plant cysteine peptidases. Molecular docking simulations confirmed the role of the catalytic triad in its proteolytic activity. Synchrotron radiation circular dichroism assays confirmed that Peruvianin-I was stable at pH ranging from 5.0 to 8.0 and that it presented significant structural changes only above 60 °C. The addition of iodoacetamide caused changes in its native conformation, but only a slight effect was observed after adding a reducing agent. This study reports an unusual protein with germin-like structure, lacking typical oxalate oxidase activity. Instead, the proteolytic activity observed suggests that the protein is a cysteine peptidase. These structural peculiarities make Peruvianin-I an interesting model for further understanding of the action of laticifer fluids in plant defense.

1. Introduction

Germins are highly conserved plant proteins that exhibit oxalate oxidase (OxO) activity, responsible for producing H_2O_2, a mediator of oxidative burst and cellular signaling, which suggests their defensive roles against biotic and abiotic stresses [1,2]. The term germins comes from the fact they were first identified from germinated wheat grains. To date, they have been described only in cereals [3]. However, proteins similar to germins have been identified, called germin-like proteins (GLPs).

GLPs have been reported in monocots, dicots, gymnosperms, and mosses [4,5]. They are very heterogeneous in amino acid sequences and this diversity can explain, at least in part, their different biochemical properties, including serine protease inhibition, ADP-glucose pyrophosphatase/phosphodiesterase, and polyphenol oxidase activity [6–8]. Recently, a new member of the germin-like protein (GLP) group, named Peruvianin-I, was identified in *Thevetia peruviana* latex. This protein was purified and characterized as a GLP due to the high identity shared with other GLPs in its N-terminus region. Interestingly, Peruvianin-I presented striking proteolytic activity, which had never been described before for any other GLP [9].

Peptidases are a group of proteins that are able to catalyze the hydrolytic cleavage of peptide bonds in proteins and peptides [10]. In plants, the biological roles of peptidases are related to senescence, initiation of cell death, protein mobilization, and seed germination [11]. In addition, peptidases can also participate in defense mechanisms against aggressors such as fungi and insects [12,13].

Considering that the GLP from *T. peruviana* latex exhibits proteolytic properties, but lacks oxalate oxidase activity, the purpose of the study was to investigate in detail its three-dimensional structure, in an attempt to understand this peculiar enzymatic activity. Peruvianin-I cDNA was cloned, sequenced, and its three-dimensional model was predicted by homology modeling, for comparison with other germins and GLPs. The active site of Peruvianin-I was analyzed by molecular docking using oxalate oxidase substrate or peptidase inhibitor. Finally, the protein was purified and its secondary structure was characterized by synchrotron radiation circular dichroism spectroscopy and its enzymatic kinetics was compared to another standard peptidase.

* Corresponding author.
E-mail address: cleversondiniz@ufc.br (C.D.T. Freitas).

https://doi.org/10.1016/j.ijbiomac.2019.01.023
0141-8130/

2. Material and methods

2.1. RNA extraction, cDNA synthesis and 3′RACE PCR

Thevetia peruviana leaves were collected, washed with distilled water and ground in liquid nitrogen to yield a fine powder. Then, the total RNA was isolated using the RNeasy Mini kit according to the manufacturer's instructions (Qiagen, Germany). The RNA was analyzed by agarose gel electrophoresis and quantified by absorbance at 260 nm. The cDNAs were synthesized from the DNA-free total RNA previously extracted by using the ImProm-II Reverse Transcription System (Promega, USA) and the 3′ RACE adapter (5′-GCGAGCACAGAATTAA TACGACTCACTATAGG$(T)_{12}$VN-3′), as described by the manufacturer (ThermoFisher Scientific, USA).

The PCR assays were performed by using the 3′ RACE outer primer (5′-GCGAGCACAGAATTAATACGACT-3′) and the specific primer designed for Peruvianin-I, the GLP from *T. peruviana* latex (5′-CCGG GCYGATCCWGGTCCHTTRCARGA-3′), called PeruvF. The N-terminus amino acid sequence of Peruvianin-I (ADPGPLQDF) and other GLPs were used to construct PeruvF (forward primer). The amplification reactions were performed in a final volume of 25 μl containing the first strand cDNA (900 ng), 200 μM dNTP, 1.5 mM $MgCl_2$, 0.5 μM primer, 2 U Taq DNA Polymerase (GE Healthcare Life Sciences, USA) and 10× the reaction buffer (GE Healthcare Life Sciences, USA). The PCR cycles were performed under the following conditions: an initial denaturation step of 2 min at 95 °C and, sequentially, 32 cycles of 45 s at 95 °C, 45 s at different temperatures (45–65 °C), and 1.5 min at 72 °C. Finally, after the last cycle the reaction mixture was incubated for 5 min at 72 °C and cooled to 4 °C. The reaction products were visualized by 1% (v/v) agarose gel electrophoresis stained with ethidium bromide (0.8 mg/ml).

2.2. Cloning and sequence analysis

PCR products were excised from the agarose gels, purified using the DNA Gel Extraction Column kit (Promega, USA), ligated into the pGEM-T Easy vector using T4 DNA ligase (Promega, USA), and then used to transform electrocompetent DH5α *Escherichia coli* cells by electroporation. The plasmid DNAs were isolated from the antibiotic resistant colonies using the NucleoSpin Plasmid kit (Macherey Nagel, Germany) and sequenced by Macrogen Inc. (Seoul, South Korea) using the primers T7 promoter and SP6. The software package Phred-Phrap-Consed-Polyphred (PPCP) was used to produce a unique consensus sequence encoding one distinct polypeptide chain [14–16].

The amino acid sequences obtained were analyzed by multiple alignments with the Clustal-W software [17] and the similarities with other proteins were determined using BLASTp [18]. The theoretical molecular mass and isoelectric point (pI) were evaluated using the ExPASy ProtParam Proteomics Server [19] and the presence of disulfide bonds was predicted by the DIANNA web server [20]. Finally, the prediction of N-glycosylation sites was evaluated using the NetNGlyc 1.0 server (http://www.cbs.dtu.dk/services/NetNGlyc/).

2.3. Phylogenetic tree and 3D models

Amino acid sequences were aligned using ClustalW with the following parameters: gap opening penalty 10 and gap extension penalty 0.2 [17]. These sequences were used to construct the phylogenetic tree employing the neighbor joining method by the MEGA 7.0 program [21]. Several plant GLP sequences were used to compare the different germin groups (Supplementary Table 1).

The protein models were formulated using different platforms: Swiss Model (https://swissmodel.expasy.org/), GalaxyWeb (http://galaxy.seoklab.org/) and M4T server v. 3.0 (manaslu. aecom.yu.edu/M4T/) [22–24]. The crystal structure of *Hordeum vulgare* germin (PDB number: 1FI2) was selected as a template [25] to build the three-dimensional models of Peruvianin-I, because both proteins share 41% sequence identity. The models were analyzed from their geometric and stereochemical quality using the PROCHECK [26] and WHAT IF [27] programs. The PyMOL software was used to analyze and visualize the three-dimensional models generated (http://pymol.org/).

2.4. Molecular docking

AutoDock 4.2 and AutoDockVina were utilized to perform the molecular docking analysis [28]. The grid maps of 40 Å × 40 Å × 40 Å were centered on the possible oxalate oxidase or proteolytic activity sites of Peruvianin-I and calculated with the AutoGrid software using germin (1FI2) and papain (1PPN) structures as templates. The molecular structures of iodoacetamide (IAA, a specific cysteine peptidase inhibitor) and oxalate (a specific substrate for oxalate oxidase activity) were obtained from the Pubchem Substance Database and used for docking calculations. Iodoacetamide and oxalate exhibited free rotation, while the protein was held rigid. The ten best structures were analyzed and ranked according to the predicted binding affinity (expressed in kcal/mol). Three-dimensional images of the interactions between ligands and the proteins were prepared using the PyMOL software.

2.5. Synchrotron radiation circular dichroism (SRCD) spectroscopy analysis

All spectrometric analyses were performed with the native Peruvianin-I, which was purified, and its proteolytic activity was confirmed by enzymatic assays using 1% azocasein as substrate at pH 6.0 [9,29]. SRCD spectroscopy was employed to investigate the structure of Peruvianin-I (instead of the conventional circular dichroism method), because of the ability to measure lower wavelength data and the improved signal-to-noise ratio of the technique. These data allow higher accuracy in determining the secondary structure of proteins with low content of helix and high content of beta conformation [30]. The SRCD spectra of Peruvianin-I (0.66 mM) in aqueous solutions were collected at the AU-CD beamline of the ASTRID2 synchrotron (Aarhus, Denmark), taking three successive scans over the wavelength range from 170 to 270 nm, in 1 nm intervals, using a 98.6 μm pathlength Suprasil quartz cuvette at 25 °C.

Additionally, a dehydrated film of Peruvianin-I (0.7 nM) was obtained on the surface of a quartz plate, by depositing the protein solution on the plate and keeping it under vacuum overnight. The SRCD spectra of the dehydrated films were obtained from 280 to 155 nm, at 25 °C, taking four different rotations on the plate (0°, 90°, 180°, and 270°) in order to avoid any linear dichroism effect.

Protein stability was investigated at different pH levels by incubating protein for 30 min in buffers: 20 mM sodium acetate (pH 4.0 and 5.0) or 20 mM sodium phosphate (pH 6.0, 7.0, and 8.0) in the presence of 1 mM dithiothreitol (DTT), a reducing agent and activator of cysteine peptidases, and taking the respective SRCD spectra. Protein at pH 6.0 was also incubated at temperatures ranging from 20 to 90 °C, in 10 °C steps, allowing 5 min equilibration at each temperature, and taking three scans at each point.

All SRCD spectra were processed using the CDTools software [31] and consisted of averaging the individual scans, subtracting the respective averaged baseline (solution containing all components of the sample, except the protein), smoothing with the Savitzky-Golay filter, zeroing at 263–270 nm, and expressing the final SRCD spectra in delta epsilon units, using a mean residual weight of 110.9. Estimation of Peruvianin-I secondary structure content was performed with the Dichroweb server [32].

To assess the role of the disulfide bridge in maintaining the secondary structure of Peruvianin-I, different concentrations of DTT (1–10 mM) were incubated at pH 6.0 with the protein at 25 °C. The influence of iodoacetamide (IAA), a cysteine peptidase inhibitor, on Peruvianin-I's structural conformation was also investigated under the same conditions. In this case, Peruvianin-I was evaluated for its structural behavior,

either in its native (free) form or complexed with IAA (10 mM) under reducing conditions (1 mM DTT) at pH 6.0.

2.6. Histochemical detection of oxalate oxidase (OxO) activity

OxO activity *in situ* was detected using the procedure of Dumas et al. [33]. Leaves of *T. peruviana*, approximately 8 × 2 cm, were incubated in a bleach solution (0.15% TCA, 75% ethanol, 25% chloroform) for 60 min, washed with distilled water, and immersed in an activation solution (40 mM succinate buffer, pH 4.0, containing 60% ethanol, 3 mM oxalic acid, 0.1 mg/ml 4-chloro-1-naphthol and 3 mM EDTA) for 60 min at 37 °C. *Oryza sativa* leaves were used as positive control for oxalate oxidase activity [34]. The appearance of blue spots in the plant tissue evidenced the oxalate oxidase activity, which was easily observed using a light microscope.

2.7. Kinetic parameters for proteolytic activity

The kinetic parameters of Peruvianin-I peptidase activity were determined at 37 °C, using Nα-Benzoyl-DL-arginine β-naphthylamide hydrochloride (BANA)(Sigma, Brazil) as specific substrate for cysteine peptidases. The reaction mixture consisted of 20 μg of Peruvianin-I (20 μl, 1 mg/ml in 50 mM sodium phosphate buffer, pH 6.0) and a final concentration of BANA ranging from 0.1 to 0.5 mM, in 50 mM sodium phosphate buffer (pH 6.0), containing 1 mM DTT. The final volume of the reaction was 500 μl. After 30 min at 37 °C, the reaction was stopped by adding 500 μl of 2% HCl in ethanol and 500 μl of 0.06% 4-(dimethyl-amino) cinnamaldehyde (Sigma, Brazil). After 40 min, the resulting yellow color was measured by absorbance at 540 nm [29]. All assays were performed in triplicate. V_m, K_m and k_{cat} were calculated using linear regression analysis based on the Lineweaver–Burk plot. Purified papain (a cysteine peptidase from *Carica papaya* latex) was used as control [35]. Statistical significance was calculated by the paired *t*-test ($p < 0.05$) using the GraphPad Prism 6 program.

3. Results and discussion

3.1. Sequence analysis of Peruvianin-I

All 10 cDNA clones obtained by 3′ RACE PCR encoded only one polypeptide sequence of 202 amino acids without signal peptide, because the forward primer used was based on the N-terminus of the mature Peruvianin-I (Fig. 1). The sequences of other germin-like proteins that share the highest identity with Peruvianin-I are shown in Fig. 1. Similar to other GLPs, Peruvianin-I has two cysteine residues located close to its N-terminal, which are involved in the formation of a disulfide bond [36,37]. Interestingly, another cysteine residue (Cys_{77}) is present solely

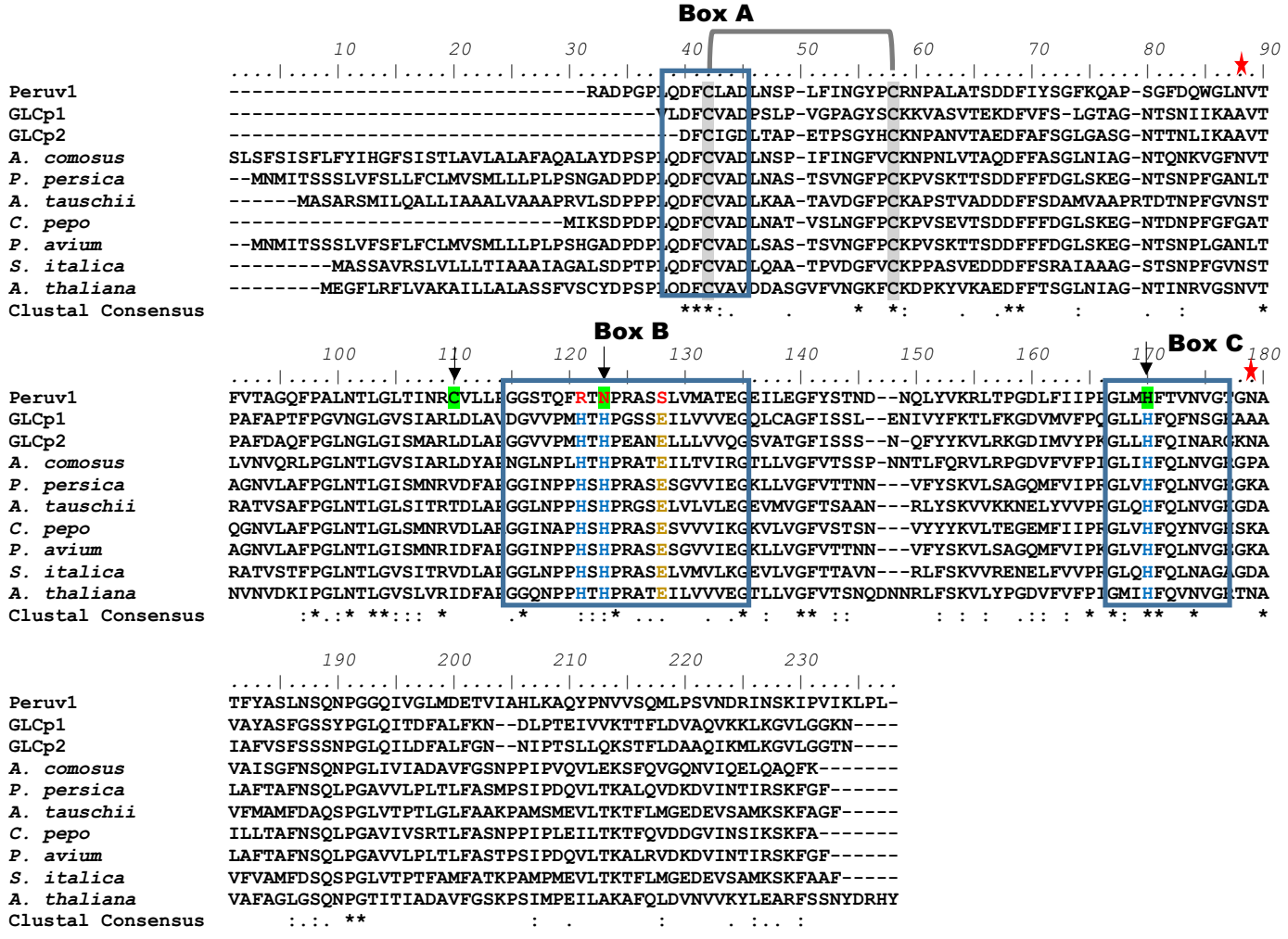

Fig. 1. Multiple sequence alignment among Peruvianin-I (Peruv1) and different germin-like proteins (GLPs). The two cysteine residues responsible for formation of a disulfide bond, which is highly conserved in all GLPs, are highlighted in gray. Putative N-glycosylation sites are marked with a red asterisk. The three histidine residues, colored in blue (box B and C), and the glutamate, in orange (box B), represent the amino acids known to be involved in oxalate oxidase activity. The amino acid residues of Peruvianin-I that were different than the amino acids of the catalytic site for oxalate oxidase in GLPs are indicated in red. The amino acids present in Peruvianin-I responsible for its proteolytic activity are highlighted in green and by arrows.

in the Peruvianin-I sequence, while all the other GLPs have predominantly a leucine or valine at the same position (Fig. 1).

Most of the germins and GLPs have highly conserved amino acid residues, located in regions denominated germin boxes A, B and C [38]. As shown in Fig. 1, Peruvianin-I exhibited these three conserved sequences. However, two His and one Glu, which are highly conserved in germin box B, are replaced in Peruvianin-I by Arg, Asn and Ser, respectively. On the other hand, other amino acids in box C, including His, were conserved in Peruvianin-I (Fig. 1). The His and Glu in box B and the His in box C are fundamental for oxalate oxidase activity of germins [39].

Two putative N-glycosylated sites were predicted in Peruvianin-I, at positions Asn_{55} and Asn_{144}, using *in silico* analysis (Fig. 1). Similarly, two N-glycosylation sites were predicted in *Calotropis procera* GLPs (Asn_{41}, Asn_{57}) and wheat germin (Asn_{47}, Asn_{52}) [40,41]. This *in silico* analysis was confirmed by previous results, since Peruvianin-I has been described as a glycoprotein with a carbohydrate content of almost 22% [9]. Asparagine N-linked glycosylation is the best known co- and post-translational modification of secretory proteins [42], and N-glycosylation is essential for many biological processes, including expression and folding of glycoprotein, glycan-dependent quality control processes in the endoplasmic reticulum (ER), and protein–protein interactions [43]. However, the specific role played by glycosylation in GLPs is still unknown.

Peruvianin-I presented a mature sequence of 202 amino acids, predicted molecular mass of 21.85 kDa and isoelectric point (pI) of 5.58 (Supplementary Table 1). These values are in concordance with those described previously [9], since analysis by SDS-PAGE showed that Peruvianin-I had an apparent molecular mass of 20 kDa, which was confirmed by mass spectrometry, which only detected peaks of approximately 20,522 Da [9]. Two-dimensional gel electrophoresis of Peruvianin-I indicated the presence of spots with molecular masses around 20 kDa and pI values between 4.0 and 5.0 [9]. These biochemical characteristics were quite similar to several other GLPs, in which the mature amino acid sequences (without signal peptides) ranged from 189 to 207 amino acids, molecular masses from 18.2 to 22.7 kDa and pI from 5.45 to 8.03 (Supplementary Table 1).

Structural analysis of several germins and GLPs permitted grouping them into ten different clades/subfamilies, namely GER 1, GER 2, GER 3, GER 4, GER 5, GER 6, GER 7, GER 8 and bryophyte subfamilies 1 and 2 [38]. The phylogenetic analysis of Peruvianin-I and several germins and GLPs (Supplementary Table 2), representing all clades/subfamilies, showed that Peruvianin-I did not belong to any classification previously described (Fig. 2). When the three amino acids from box B in Peruvianin-I (Arg, Asn and Ser) were replaced by two His and one Glu (amino acids conserved in germin and GLPs), Peruvianin-I was included in clade GER 2, similar to GLPs from *C. procera* latex [40]. These results show that Peruvianin-I should be classified in a new clade/subfamily of GLPs. Therefore, we suggest a new clade/subfamily named GER 9, in which GLPs exhibiting activities other than oxalate oxidase should be gathered, such as serine protease inhibition, ADP-glucose pyrophosphatase/phosphodiesterase and polyphenol oxidase activity, besides proteolytic activity [6–9].

3.2. Prediction of the active site for oxalate oxidase activity in Peruvianin-I

The three-dimensional models of Peruvianin-I were obtained by homology modeling using *H. vulgare* germin (PDB number: 1FI2) as a template. The Ramachandran plot and the analysis performed by the PROCHECK and WHAT IF servers showed that the best models were those generated by the GalaxyWeb platform (Supplementary Table 3). Structural comparisons between the overall structure of Peruvianin-I and the template revealed a RMSD of 3.428 Å. Crystallographic studies of barley germin showed that oxalate oxidase activity requires a manganese center buried in its β-barrel jellyroll domain which is bound by the side chains of three histidines and one glutamate residue (His_{88}, His_{90}, Glu_{95} and His_{137}) (Fig. 3A), forming a trigonal bipyramidal geometry [25]. Specifically, for the active site the Peruvianin-I three-dimensional model and germin crystal structure showed RSMD of 0.504 Å. The manganese ion was not bound in the Peruvianin-I β-barrel jellyroll domain, because it has the residues Arg_{88}, Asn_{90}, Ser_{95} and His_{135} instead of His_{88}, His_{90}, Glu_{95} and His_{135} (Fig. 3B). In another study, *in silico* analysis showed that the exchange of one histidine (His_{102}) by one tyrosine, in germin box B of SlGLP (*Solanum lycopersicum*), modified the architecture of the active site for Mn^{2+}. Consequently, the protein did not exhibit oxalate oxidase activity [44]. These results provide further evidence that the three histidines and glutamate are essential for oxalate oxidase activity, being responsible for correct interaction of the active site of the oxalate substrate [36]. These findings corroborate our previous results that showed Peruvianin-I does not have oxalate oxidase activity *in vitro* [9].

Molecular docking calculations using the oxalate substrate were also performed to better understand the function of four conserved amino acids in germins (His, His, Glu and His) for oxalate oxidase activity. A careful inspection of the active site of barley germin (1FI2) indicated that oxalate substrate adapted itself in a cage surrounded by His_{88}, His_{90}, Glu_{95} and His_{137}, with calculated interaction energy of $-4.1\ kcal \cdot mol^{-1}$ (Fig. 3C). As expected, the oxalate ligand interacted strongly with residues responsible for manganese ion binding. The two histidines (His_{88} and His_{90}) present in the central cores of the ß-barrel of barley germin formed two hydrogen bonds with oxalate. The bonds were between the OH group of oxalate and the N atoms from imidazole rings of His_{88} (2.0 Å) and His_{90} (2.6 Å) (Fig. 3C). By comparison, the oxalate substrate was docked only at an α-helical C-terminus domain of Peruvianin-I (Fig. 3D). As pointed out before, three residues present in the active site of barley germin were not conserved in Peruvianin-I (Fig. 1), and these changes undoubtedly influenced the binding pattern with the oxalate substrate. The hydrophobic surrounding of the active site of germin is also very important for oxalate oxidase activity [45]. Substitution of the Val_{77} and Phe_{153} residues present in barley germin (1FI2) by less hydrophobic residues (Cys_{77} and Leu_{151}) in the Peruvianin-I also negatively influenced the interaction with the oxalate. Accordingly, it was shown that the decrease of nonpolar residues in the active site of *Arabidopsis* GLP significantly decreased its interaction with the oxalate [45].

Thevetia peruviana leaves were used to detect possible *in situ* activity of oxalate oxidase, since purified Peruvianin-I can lose its activity during the purification process [9]. No oxalate oxidase activity was detected in *T. peruviana* leaves, in contrast to *Oryza sativa* leaves, used as positive control (Fig. 4). This result corroborates those from *in silico* analysis and supports that Peruvianin-I does not have oxalate oxidase activity.

3.3. Characterization of the active site for proteolytic activity of Peruvianin-I

Although previous results showed that Peruvianin-I is a cysteine peptidase, its structural characterization was not performed [9]. Based on the primary and tertiary structures of Peruvianin-I, it was possible to observe that it contains the same catalytic triad (Cys_{77}, Asn_{90} and His_{135}) present in the structure of several cysteine peptidases, including papain (Cys_{25}, His_{159} and Asn_{175}) (Fig. 5). Interestingly, these results show that Peruvianin-I underwent punctual mutations, which were responsible for the loss of oxalate oxidase activity while at the same time exhibiting proteolytic activity (Fig. 1). The structural overlap shows that the active-site architecture and the spatial arrangement of amino acid residues involved in enzyme catalysis of papain are reasonably similar to Peruvianin-I residues (Fig. 5C), which are located within its β-barrel jellyroll domain (Fig. 5B).

Most plant cysteine peptidases belong to the papain (C1) and legumain (C13) families. All these peptidases have a nucleophilic cysteine thiol in their catalytic triad (Cys, His, and Asn) [46]. Interestingly, Peruvianin-I presents a similar spatial arrangement of the catalytic triad responsible for this proteolytic activity, despite having completely different structural domains than proteins belonging to the papain

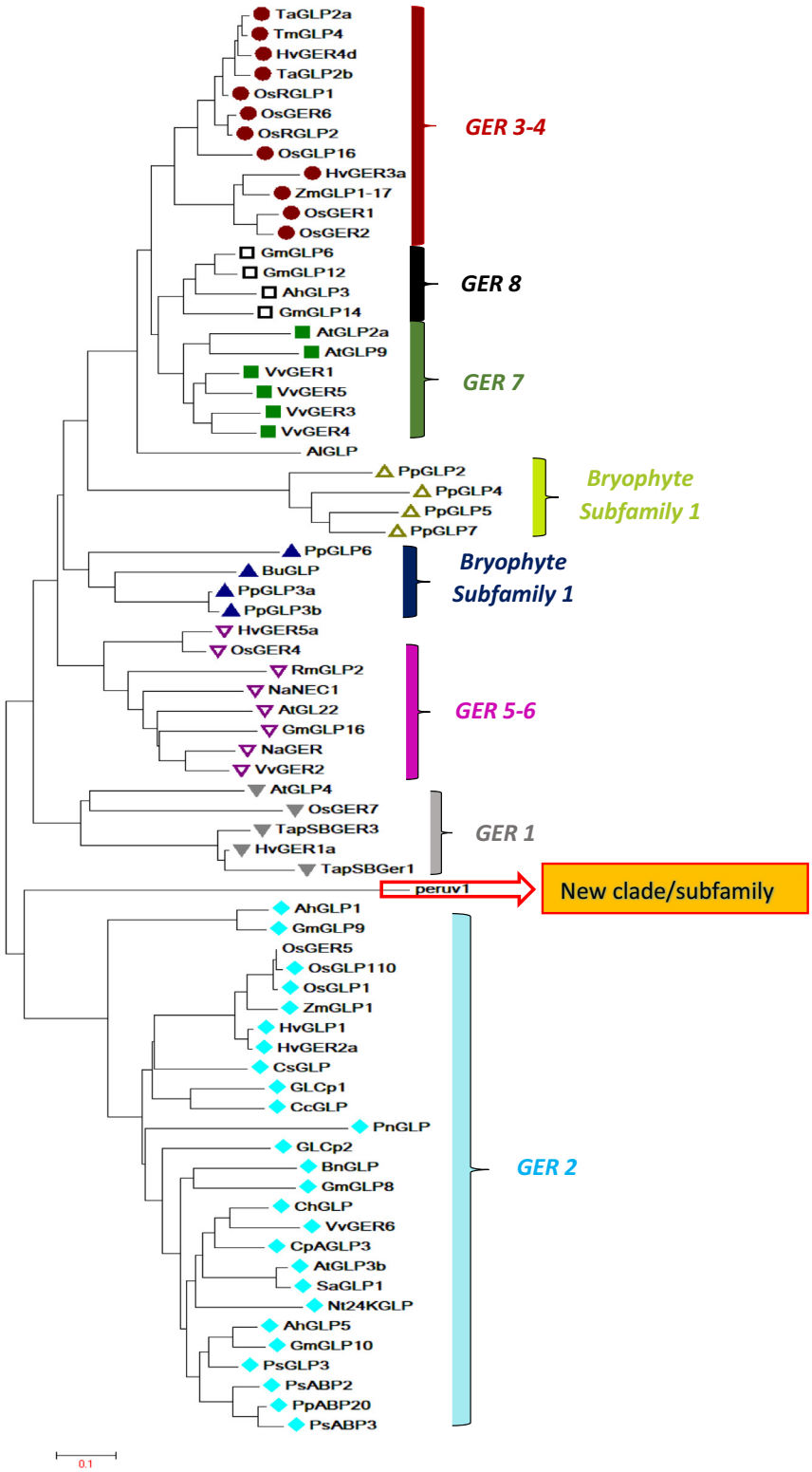

Fig. 2. Phylogenetic analyses of Peruvianin-I and other plant GLPs. The phylogenetic tree was constructed with the neighbor-joining algorithm using MEGA 7 software. The clades/subfamilies were organized into different symbols and colors. Peruvianin-I, a member of a new clade/subfamily, is highlighted by the red arrow. The GenBank accession numbers of the sequences analyzed are available in Supplementary Table 2.

family. The molecular docking analysis between cysteine peptidase inhibitor (iodoacetamide, IAA) and papain (1PPP) showed that IAA forms hydrogen bonds of 2.2 Å and 2.9 Å with Gln_{19} and His_{159} residues, respectively, as well as having interaction energy of -3.5 kcal·mol^{-1} (Fig. 6A). In Peruvianin-I, there was one hydrogen bond between the nitrogen of the imidazole ring of His_{135} and IAA, with a mean distance of 2.6 Å, and another one between IAA and the residue of Cis_{77}, with total energy of -2.9 kcal·mol^{-1} (Fig. 6B). This interaction was confirmed when the proteolytic activity of Peruvianin-I was totally and specifically inhibited by IAA [9]. The interaction between IAA and cysteine peptidases generates an alkylation reaction between the iodine group of the inhibitor and the sulfur group of the cysteine residue of the

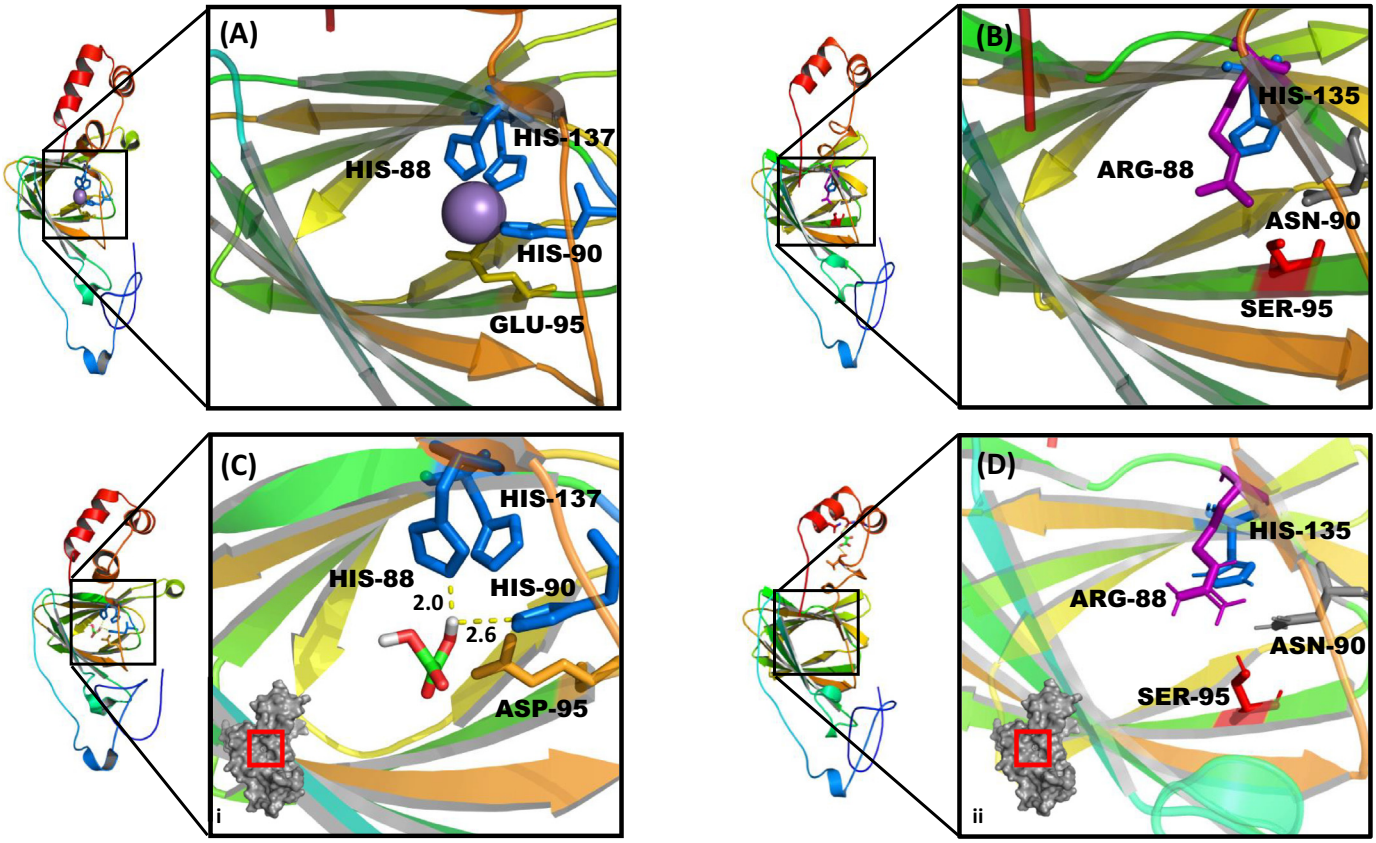

Fig. 3. Comparison of the active site of the barley germin (1FI2) and of the three-dimensional model of Peruvianin-I related to the oxalate oxidase activity, as well as the molecular docking of these structures against the ligand oxalate (substrate for oxalate oxidase activity). (A) Four amino acids involved in the oxalate oxidase activity of the barley germin and their interaction with Mn^{2+} ion. (B) In these same positions, different residues (Arg_{88}, Asn_{90}, Ser_{95}) are present in the structure of Peruvianin-I. (C) Molecular docking simulation of the interactions between oxalate and barley germin. (D) The lack of residues responsible for oxalate oxidase activity in Peruvianin-I generated no coupling of the ligand oxalate. Interaction distances between oxalate and residues are given in Å units.

catalytic triad, forming a stable thioether bond [47]. This reaction results in a very stable enzyme–inhibitor complex, which is responsible for irreversible inhibition of peptidases [9].

The proteolytic activity of Peruvianin-I and papain followed Michaelis-Menten kinetics (Fig. 7). The k_m of Peruvianin-I, using BANA as substrate, was 0.237 ± 0.05 mM, almost four times smaller than papain, 0.809 ± 0.08 mM ($p < 0.05$). The V_{max} and K_{cat} values were 0.54×10^{-9} M·s^{-1} and 0.1 ± 0.02 s^{-1} and 9.2×10^{-9} M·s^{-1} and 2 ± 0.05 s^{-1} for Peruvianin-I and papain, respectively ($p < 0.05$). The catalytic efficiency of papain ($K_{cat}/K_m = 2.4 \times 10^4$) was about 60-fold higher than that of Peruvianin-I ($K_{cat}/K_m = 4.2 \times 10^2$). Although Peruvianin-I has the same catalytic triad, its overall and active site structures are very different from most plant cysteine peptidases, including papain. In addition, the presence of polar residues such as Ser_{95} and Arg_{88} possibly decreased the hydrophobic interaction between the catalytic site of Peruvianin-I and the hydrophobic rings of BANA. Accordingly, replacing some amino acids at the Ervatamin C active site drastically altered its catalytic efficiency [48,49]. These results clearly demonstrate that the kinetic performance of an enzyme is not strictly related to the amino acid composition of its catalytic clefts, but is closely related to the protein's adjacent residues and overall structure.

A previous study showed that Peruvianin-I exhibited no antifungal activity on different phytopathogens and that the lack of antifungal effect could be correlated to its low proteolytic activity compared to other (latex) antifungal cysteine peptidases, such as papain [9]. As pointed out before, the low proteolytic activity may be associated with its unusual germin-like tridimensional structure, which is far from the typical structure of cysteine peptidases so far described. Latex cysteine peptidases have also been related to plant defense against insects [50]. Therefore, the possible role played by Peruvianin-I in latex physiology is unclear and deserves more research.

3.4. Effect of pH, temperature, reducing agent and peptidase inhibitor on structure of Peruvianin-I

The SRCD spectrum of Peruvianin-I in aqueous solution (pH 6.0) was typical of a β-rich protein, displaying a broad negative band with small magnitude at 217 nm, and a large positive maximum at 197 nm. Since the SRCD method was employed, an additional large negative band was observed at 175 nm, which is also characteristic of the β-strand structure. These spectral features are commonly observed in proteins with elevated concentrations of β-sheet segments [51,52]. Similar SRCD spectra were observed for native Peruvianin-I independent of pH conditions (Fig. 8A). Although at pH 4.0 a small increase in the peak at 197 nm was observed, the protein's structural content was unchanged from pH 5.0 to 8.0.

The estimation of the secondary structural content of Peruvianin-I from its SRCD spectrum at 25 °C was 35% organized in β-strands, 40% disordered, plus a small content of α-helices (~9%). These results are similar to previous results of molecular modeling (Fig. 3), and are in agreement with the structural content observed in germins and GLPs [25,36,53], which are usually characterized by a beta-barrel core structure.

The SRCD spectra of the Peruvianin-I subjected to the temperature denaturation assay showed only slight changes in the range from 20 to 50 °C (Fig. 8B), revealing protein thermal stability within these temperatures. But band shifts and a significant signal reduction were seen between 60 and 70 °C, and the protein assumed a completely unfolded

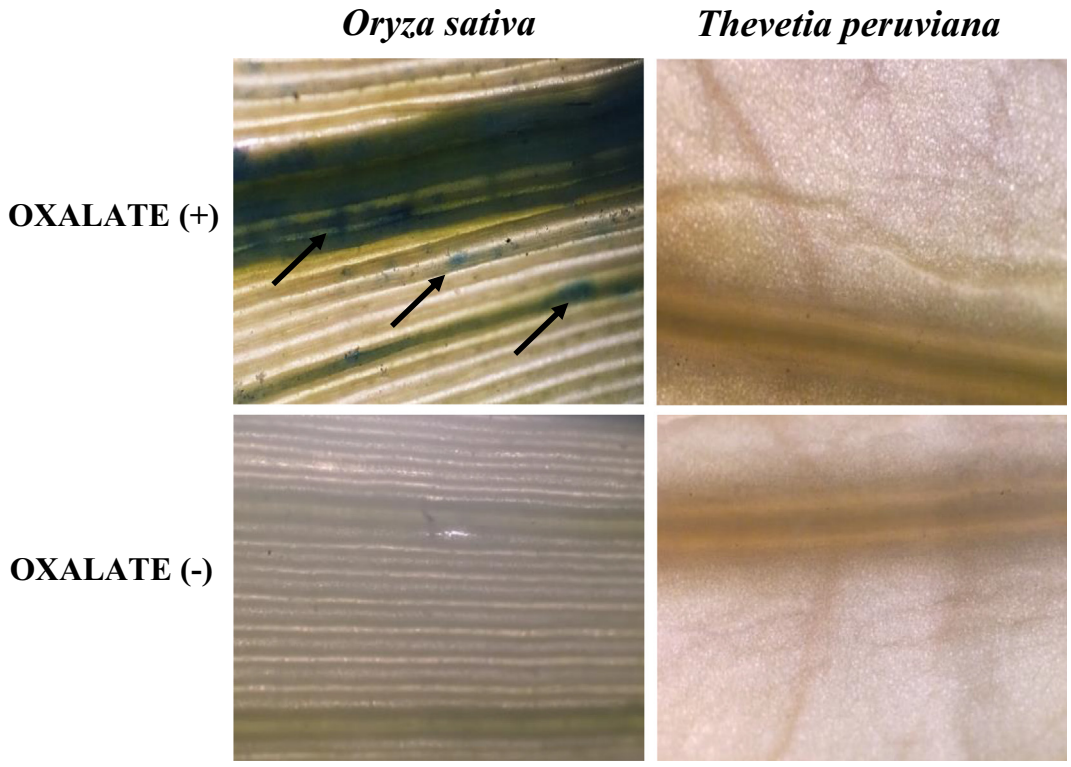

Fig. 4. *In situ* location of oxalate oxidase activity in *Thevetia peruviana* leaves. Presence (+) and absence (−) of substrate oxalate. The leaves were incubated for 2 h in the activation solution at 25 °C (see Material and Methods). The blue dots, indicated by some black arrows, show the presence of activity. Leaves of *Oryza sativa* were used as positive control. The analyses were performed under a light microscope (40× magnification).

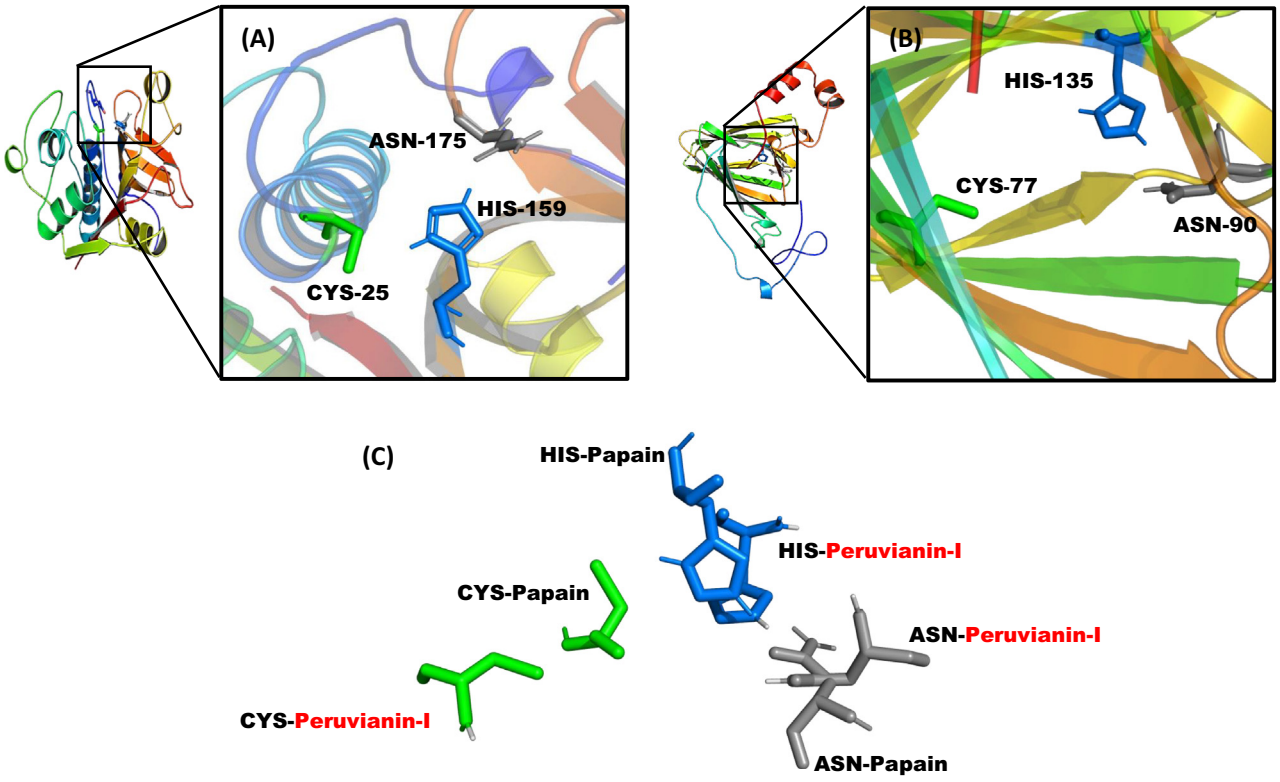

Fig. 5. Comparison of the catalytic site for cysteine proteolytic activity of papain (1PPP) and Peruvianin-I. (A) Amino acids (histidine, asparagine and cysteine) involved in the proteolytic activity of papain (A) and Peruvianin-I (B). (C) Structural overlap between the residues of the catalytic site of papain and Peruvianin-I.

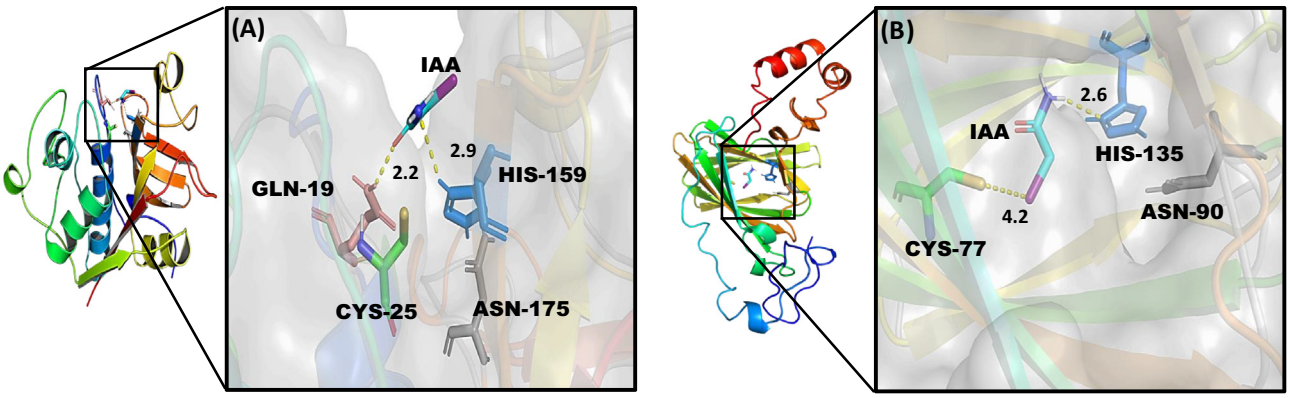

Fig. 6. Molecular docking evidencing the amino acid residues involved in the cysteine proteolytic activity of papain (A) and Peruvianin-I (B) and their interaction with the cysteine peptidase inhibitor iodoacetamide (IAA).

state at 80 and 90 °C. These results corroborate those from *in vitro* assays, where Peruvianin-I was 100% active until 45 °C and then was completely inactive at 65 °C [9].

The presence of the reducing agent DTT at concentrations of 1–10 mM (Fig. 8C) produced the same discrete change in the SRCD spectra of Peruvianin-I, with an increase of the peak at 197 nm and narrowing of the negative band at 217 nm, without changing the spectrum's typical profile. These changes can be associated with the disruption of the disulfide bridge located in the protein's N-terminus portion (Fig. 1). Because the disulfide bond is located far from the active site, its disruption did not significantly change the protein structure and its proteolytic activity remained stable [9].

In addition to analysis of SRCD in solution, the deposition of Peruvianin-I on partially dehydrated films allowed collecting data at even smaller wavelengths, close to 155 nm, adding more transitions to be monitored and further converted into structural information. The SRCD spectra of the Peruvianin-I on the film kept all the spectral bands seen in the solution and showed the full negative peak at 175 nm and a positive peak at 160 nm, both in the presence of the beta-strands. The SRCD spectra of Peruvianin-I on the film in the presence of DTT or DTT and IAA are also shown in Fig. 8D. Once again, it can be seen that DTT alone did not cause any significant structural change in Peruvianin-I. However, when IAA was added, a drastic reduction of the peaks attributed to the beta-content was seen, revealing a loss of its native conformation that affected its enzymatic activity. Similar spectroscopic studies performed with papain revealed that the alkylation of the thiol group in its active site caused changes in its secondary structure [54]. In another study, the use of iodoacetamide (IAA) modified the structure of ficin, a cysteine peptidase, and also inhibited its activity irreversibly, generating large amounts of protein aggregate [55]. Several studies have shown that iodoacetamide can cause rapid aggregation of cellular proteins [56].

4. Conclusion

Peruvianin-I is the only germin-like protein (GLP) described as having proteolytic activity. We showed that it has primary, secondary and tertiary structures very similar to other germins and GLPS. However, it underwent punctual mutations in three amino acid residues, which were responsible for the absence of the oxalate oxidase activity. On the other hand, some of these mutations together with the presence of a single free cysteine residue were responsible for forming a catalytic triad, which was highly conserved in papain-like cysteine peptidases. SRCD results confirmed the native state of Peruvianin-I and its classification as a β-rich protein, and agreed with previous proteolytic assays, in which Peruvianin-I exhibited thermostability until 50 °C and an optimal pH stability ranging from 5.0 to 7.0. Furthermore, the protein interacted with and had its secondary structure significantly changed in the presence of a cysteine peptidase inhibitor. The involvement of Peruvianin-I in latex functionalities still deserves more investigation. The structure of the protein reveled highly punctual replacements of key amino acid

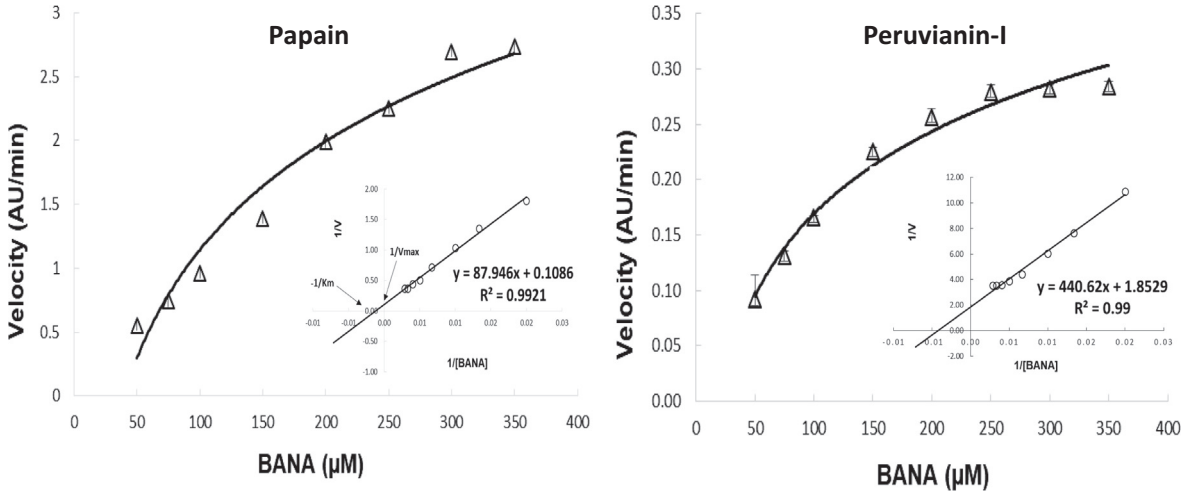

Fig. 7. Effect of substrate concentration (BANA) on proteolytic activity of papain and Peruvianin-I at pH 6.0 and 37 °C. Inset: Lineweaver-Burk plot. K_m and V_{max} were calculated from the Lineweaver-Burk plot.

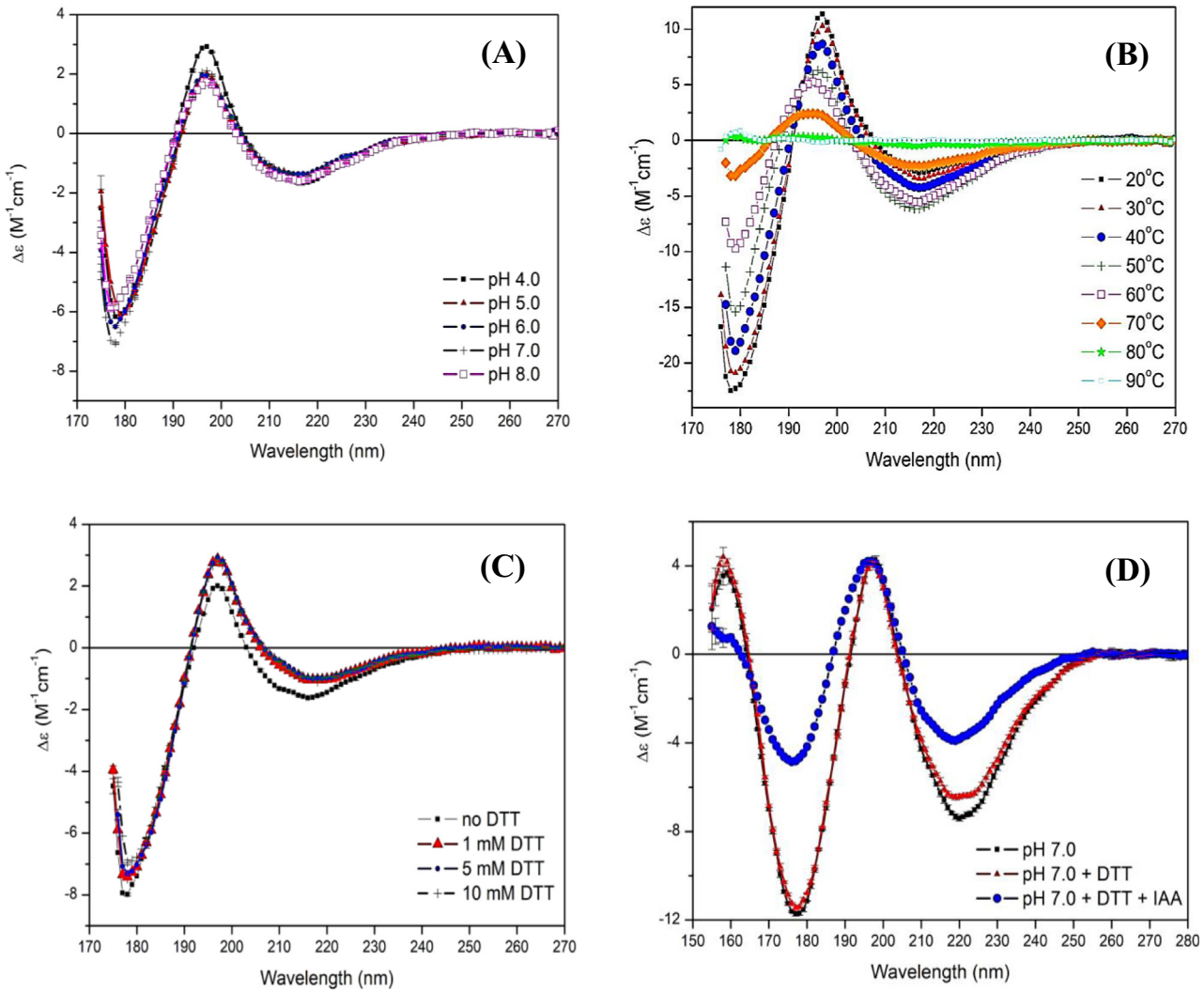

Fig. 8. Synchrotron radiation circular dichroism (SRCD) spectra of Peruvianin-I at pH ranging from 4.0 to 8.0 (A); effect of temperature (from 20 to 90 °C) on the conformation of Peruvianin-I (B); SRCD spectra of the protein in the presence of the reducing agent DTT (at 1, 5, or 10 mM) (C); and SRCD spectra of partially dehydrated films of Peruvianin-I deposited on quartz-glass plates (D) in the absence or presence of DTT (1 mM), and the influence of a cysteine peptidase inhibitor iodoacetamide (IAA, 10 mM).

residues, suggesting shift of protein activity. Whether these new features are involved in new physiological roles remains to be answered.

Conflict of interest

The authors confirm that the contents of this article pose no conflicts of interest.

Contributions

WTC, MVR, BAMR, EHSB and CDTF performed the main research work, including peptidase purification, enzymatic assays and bioinformatic analyses. WTC, MZRS, JSO, DCF and TBG performed RNA isolation, cDNA synthesis, amplification and cloning. JLSL performed all the SRCD assays. All authors contributed to data analysis, discussion and writing of the manuscript.

Funding

This work was supported by grants from the following Brazilian agencies: Conselho Nacional de Desenvolvimento Científico e Tecnológico (CNPq): grants 303513/2016-0 and 406429/2016-2 to JLSL; Coordenação de Aperfeiçoamento de Pessoal de Nível Superior (CAPES); and Fundação Cearense de Apoio ao Desenvolvimento Científico e Tecnológico (FUNCAP). We are grateful for the access to the AU-CD beamline on ASTRID2 at ISA Synchrotron (Aarhus, Denmark) (to JLSL). This study is part of the consortium "Molecular Biotechnology of Plant Latex".

Appendix A. Supplementary data

Supplementary data to this article can be found online at https://doi.org/10.1016/j.ijbiomac.2019.01.023.

References

[1] V.C. Beracochea, N.I. Almasia, L. Peluffo, V. Nahirñak, E.H. Hopp, Sunflower germin-like protein HaGLP1 promotes ROS accumulation and enhances protection against fungal pathogens in transgenic *Arabidopsis thaliana*, Plant Cell Rep. 34 (2015) 1717–1733, https://doi.org/10.1007/s00299-015-1819-4.

[2] Y. Zhang, X. Wang, X. Chang, M. Sun, Y. Zhang, W. Li, Y. Li, Overexpression of germin-like protein GmGLP10 enhances resistance to *Sclerotinia sclerotiorum* in transgenic tobacco, Biochem. Biophys. Res. Commun. 497 (2018) 160–166, https://doi.org/10.1016/j.bbrc.2018.02.046.

[3] R.M. Davidson, P.A. Reeves, P.M. Manosalva, J.E. Leach, Germins: a diverse protein family important for crop improvement, Plant Sci. 177 (2009) 499–510, https://doi.org/10.1016/j.plantsci.2009.08.012.

[4] J. Breen, M. Bellgard, Germin-like proteins (GLPs) in cereal genomes: gene clustering and dynamic roles in plant defence, Funct. Integr. Genomics 10 (2010) 463–476, https://doi.org/10.1007/s10142-010-0184-1.

[5] M. Ilyas, A. Rasheed, Functional characterization of germin and germin-like protein genes in various plant species using transgenic approaches, Biotechnol. Lett. 38 (2016) 1405–1421, https://doi.org/10.1007/s10529-016-2129-9.

[6] A.Y. Mansilla, C.I. Segarra, R.D. Conde, Structural and functional features of a wheat germin-like protein that inhibits trypsin, Plant Mol. Biol. Report. 30 (2012) 624–632, https://doi.org/10.1007/s11105-011-0372-8.

[7] M. Rodriguez-Lopez, E. Baroja-Fernandez, A. Zandueta-Criado, B. Moreno-Bruna, F.J. Munoz, T. Akazawa, J. Pozueta-Romero, Two isoforms of a nucleotide-sugar pyrophosphatase/phosphodiesterase from barley leaves (*Hordeum vulgare* L.) are distinct oligomers of HvGLP1, a germin-like protein, FEBS Lett. 490 (2001) 44–48, https://doi.org/10.1016/S0014-5793(01)02135-4.

[8] X. Cheng, X. Huang, S. Liu, M. Tang, W. Hu, S. Pan, Characterization of germin-like protein with polyphenol oxidase activity from *Satsuma mandarine*, Biochem. Biophys. Res. Commun. 449 (2014) 313–318, https://doi.org/10.1016/j.bbrc.2014.05.027.

[9] C.D.T. Freitas, W.T. Cruz, M.Z.R. Silva, I.M. Vasconcelos, F.B.M.B. Moreno, R.A. Moreira, A.C.O. Monteiro-Moreira, L.M.R. Alencar, J.S. Sousa, B.A.M. Rocha, M.V. Ramos, Proteomic analysis and purification of an unusual germin-like protein with proteolytic activity in the latex of *Thevetia peruviana*, Planta 243 (2016) 1115–1128, https://doi.org/10.1007/s00425-016-2468-8.

[10] N.D. Rawlings, Biochimie peptidase specificity from the substrate cleavage collection in the MEROPS database and a tool to measure cleavage site conservation, Biochimie 122 (2016) 5–30, https://doi.org/10.1016/j.biochi.2015.10.003.

[11] A. Schaller, A cut above the rest: the regulatory function of plant proteases, Planta 220 (2004) 183–197, https://doi.org/10.1007/s00425-004-1407-2.

[12] K. Ekchaweng, E. Evangelisti, S. Schornack, M. Tian, N. Churngchow, The plant defense and pathogen counter defense mediated by *Hevea brasiliensis* serine protease HbSPA and *Phytophthora palmivora* extracellular protease inhibitor PpEPI10, PLoS One 12 (2017), e0175795. https://doi.org/10.1371/journal.pone.0175795.

[13] M.K. Jashni, R. Mehrabi, J. Collemare, C.H. Mesarich, P.J.G.M. de Wit, The battle in the apoplast: further insights into the roles of proteases and their inhibitors in plant – pathogen, Front. Plant 6 (2015) 1–7, https://doi.org/10.3389/fpls.2015.00584.

[14] B. Ewing, P. Green, Base-calling of automated sequencer traces using Phred. II. Error probabilities, Genome Res. 8 (1998) 186–194, https://doi.org/10.1101/gr.8.3.186.

[15] B. Ewing, L. Hillier, M.C. Wendl, P. Green, Base-calling of automated sequencer traces using Phred. I. Accuracy assessment, Genome Res. 8 (1998) 175–185, https://doi.org/10.1101/gr.8.3.175.

[16] D. Gordon, C. Abajian, P. Green, Consed: a graphical tool for sequence finishing, Genome Res. 8 (1998) 195–202, https://doi.org/10.1101/gr.8.3.195.

[17] J.D. Thompson, D.G. Higgins, T.J. Gibson, CLUSTALW: improving the sensitivity of progressive multiple sequence alignment through sequence weighting, position-specific gap penalties and weight matrix choice, Nucleic Acids Res. 22 (1994) 4673–4680.

[18] S.F. Altschul, W. Gish, W. Miller, E.W. Myers, D.J. Lipman, Basic local alignment search tool, J. Mol. Biol. 215 (1990) 403–410, https://doi.org/10.1016/S0022-2836(05)80360-2.

[19] M.R. Wilkins, E. Gasteiger, A. Bairoch, J.C. Sanchez, K.L. Williams, R.D. Appel, D.F. Hochstrasser, Protein identification and analysis tools in the ExPASy server, Methods Mol. Biol. 112 (1999) 531–552.

[20] F. Ferrè, P. Clote, DiANNA: a web server for disulfide connectivity prediction, Nucleic Acids Res. 33 (2005) W230–W232, https://doi.org/10.1093/nar/gki412.

[21] S. Kumar, G. Stecher, K. Tamura, MEGA: molecular evolutionary genetics analysis version 7.0 for bigger datasets, Mol. Biol. Evol. 33 (2017) 1870–1874, https://doi.org/10.1093/molbev/msw054.

[22] L. Bordoli, F. Kiefer, K. Arnold, P. Benkert, J. Battey, T. Schwede, Protein structure homology modeling using SWISS-MODEL workspace, Nat. Protoc. 4 (2009) 1–13, https://doi.org/10.1038/nprot.2008.197.

[23] J. Ko, H. Park, L. Heo, C. Seok, GalaxyWEB server for protein structure prediction and refinement, Nucleic Acids Res. 40 (2012) 294–297, https://doi.org/10.1093/nar/gks493.

[24] N. Fernandez-fuentes, C.J. Madrid-aliste, B.K. Rai, J.E. Fajardo, A. Fiser, M4T: a comparative protein structure modeling server, Nucleic Acids Res. 35 (2007) 363–368, https://doi.org/10.1093/nar/gkm341.

[25] O. Opaleye, R.S. Rose, M.M. Whittaker, E.J. Woo, J.W. Whittaker, R.W. Pickersgill, Structural and spectroscopic studies shed light on the mechanism of oxalate oxidase, J. Biol. Chem. 281 (2006) 6428–6433, https://doi.org/10.1074/jbc.M510256200.

[26] R.A. Laskowski, M.W. Macarthur, D.S. Moss, J.M. Thornton, PROCHECK: a program to check the stereochemical quality of protein structures, J. Appl. Crystallogr. 26 (1993) 283–291.

[27] G. Vriend, WHAT IF: a molecular modeling and drug design program, J. Mol. Graph. 8 (1990) 52–56.

[28] O. Trott, A.J. Olson, AutoDock Vina: improving the speed and accuracy of docking with a new scoring function, efficient optimization and multithreading, J. Comput. Chem. 31 (2011) 455–461, https://doi.org/10.1002/jcc.21334.AutoDock.

[29] C.D.T. Freitas, J.S. Oliveira, M.R.A. Miranda, N.M.R. Macedo, M.P. Sales, L.A. Villas-Boas, M.V. Ramos, Enzymatic activities and protein profile of latex from *Calotropis procera*, Plant Physiol. Biochem. 45 (2007) 781–789, https://doi.org/10.1016/j.plaphy.2007.07.020.

[30] P.S. Kumagai, R. Demarco, J.L.S. Lopes, Advantages of synchrotron radiation circular dichroism spectroscopy to study intrinsically disordered proteins, Eur. Biophys. Soc. Assoc. 46 (2017) 599–606, https://doi.org/10.1007/s00249-017-1202-1.

[31] J.G. Lees, B.R. Smith, F. Wien, A.J. Miles, B.A. Wallace, CDtool — an integrated software package for circular dichroism spectroscopic data processing, analysis, and archiving, Anal. Biochem. 332 (2004) 285–289, https://doi.org/10.1016/j.ab.2004.06.002.

[32] L. Whitmore, B.A. Wallace, Protein secondary structure analyses from circular dichroism spectroscopy: methods and reference databases, Biopolymers 89 (2008) 392–400, https://doi.org/10.1002/bip.20853.

[33] B. Dumas, G. Freyssinet, K.E. Pallett, Tissue-specific expression of germin-like oxalate oxidase during development and fungal infection of barley seedlings, Plant Physiol. 107 (1995) 1091–1096, https://doi.org/10.1104/pp.107.4.1091.

[34] X.Y. Zhang, Z.H. Nie, W.J. Wang, D.W. Leung, D.G. Xu, B.L. Chen, Z. Chen, L.X. Zeng, E.E. Liu, Relationship between disease resistance and rice oxalate oxidases in transgenic rice, PLoS One 24 (2013), e78348. https://doi.org/10.1371/journal.pone.0078348.

[35] M. Azarkan, A. Moussaoui, D. Wuytswinkel, G. Dehon, Y. Looze, Fractionation and purification of the enzymes stored in the latex of *Carica papaya*, J. Chromatogr. B 790 (2003) 229–238, https://doi.org/10.1016/S1570-0232(03)00084-9.

[36] E. Woo, J.M. Dunwell, P.W. Goodenough, A.C. Marvier, R.W. Pickersgill, Germin is a manganese containing homohexamer with oxalate oxidase and superoxide dismutase activities, Nat. Struct, Biology (2000) 7, https://doi.org/10.1038/80954.

[37] X. Chen, M.L. Wang, C. Holbrook, A. Culbreath, X. Liang, Identification and characterization of a multigene family encoding germin-like proteins in cultivated peanut (*Arachis hypogaea* L.), Plant Mol. Biol. Report. 29 (2011) 389–403, https://doi.org/10.1007/s11105-010-0237-6.

[38] A.R. Barman, J. Banerjee, Versatility of germin-like proteins in their sequences, expressions, and functions, Funct. Integr. Genomics 15 (2015) 533–548, https://doi.org/10.1007/s10142-015-0454-z.

[39] A. Sakamoto, T. Nishimura, Y. Miyaki, S. Watanabe, H. Takagi, S. Izumi, H. Shimada, In vitro and in vivo evidence for oxalate oxidase activity of a germin-like protein from azalea, Biochem. Biophys. Res. Commun. 458 (2015) 536–542, https://doi.org/10.1016/j.bbrc.2015.02.002.

[40] C.D.T. Freitas, D.C. Freitas, W.T. Cruz, C.T.M.N. Porfírio, M.Z.R. Silva, J.S. Oliveira, C. Paiva, S. Carvalho, M.V. Ramos, Identification and characterization of two germin-like proteins with oxalate oxidase activity from *Calotropis procera latex*, Int. J. Biol. Macromol. 105 (2017) 1051–1061, https://doi.org/10.1016/j.ijbiomac.2017.07.133.

[41] H.Y. Pan, M.N. Whittaker, R. Bouveret, A. Berna, F. Bernier, J.W. Whittaker, Characterization of wheat germin (oxalate oxidase) expressed by *Pichia pastoris*, Biochem. Biophys. Res. Commun. 356 (2007) 925–929, https://doi.org/10.1016/j.bbrc.2007.03.097.

[42] R. Strasser, Plant protein glycosylation, Glycobiology 26 (2016) 926–939, https://doi.org/10.1093/glycob/cww023.

[43] D.N. Hebert, L. Lamriben, E.T. Powers, J.W. Kelly, The intrinsic and extrinsic effects of N-linked glycans on glycoproteostasis, Nat. Chem. Biol. 10 (2014) 902, https://doi.org/10.1038/nchembio.1651.

[44] T. Chattopadhyay, In silico analysis of the germin like protein multigene family members of tomato with predicted oxalate oxidase activity, Int. J. Agric. Environ. Biotechnol 7 (2014) 669–678, https://doi.org/10.5958/2230-732X.2014.01374.6.

[45] C.N. Khobragade, S.D. Beedkar, R.G. Bodade, A.S. Vinchurkar, Comparative structural modeling and docking studies of oxalate oxidase: possible implication in enzyme supplementation therapy for urolithiasis, Int. J. Biol. Macromol. 48 (2011) 466–473, https://doi.org/10.1016/j.ijbiomac.2011.01.007.

[46] M. Díaz-Mendoza, B. Velasco-Arroyo, P. González-Melendi, M. Martínez, I. Díaz, C1A cysteine protease-cystatin interactions in leaf senescence, J. Exp. Bot. 65 (2014) 3825–3833, https://doi.org/10.1093/jxb/eru043.

[47] M.T.R. Gomes, H.A. Ribeiro, M.T.P. Lopes, F. Guzman, C.E. Salas, Biochemical comparison of two proteolytic enzymes from *Carica candamarcensis*: structural motifs underlying resistance to cystatin inhibition, Phytochemistry 71 (2010) 524–530, https://doi.org/10.1016/j.phytochem.2009.12.018.

[48] R. Ghosh, S. Chakraborty, C. Chakrabarti, J.K. Dattagupta, S. Biswas, Structural insights into the substrate specificity and activity of ervatamins, the papain-like cysteine proteases from a tropical plant, *Ervatamia coronaria*, FEBS J. 275 (2008) 421–434, https://doi.org/10.1111/j.1742-4658.2007.06211.x.

[49] S. Dutta, J.K. Dattagupta, S. Biswas, Enhancement of proteolytic activity of a thermostable papain-like protease by structure-based rational design, PLoS One 8 (2013), e62619. https://doi.org/10.1371/journal.pone.0062619.

[50] K. Konno, Plant latex and other exudates as plant defense systems: roles of various defense chemicals and proteins contained therein, Phytochemistry 72 (2011) 1510–1530, https://doi.org/10.1016/j.phytochem.2011.02.016.

[51] J.T. Pelton, L.R. Mclean, Spectroscopic methods for analysis of protein secondary structure, Anal. Biochem. 176 (2000) 167–176, https://doi.org/10.1006/abio.1999.4320.

[52] L. Whitmore, B.A. Wallace, Protein secondary structure analyses from circular dichroism spectroscopy: methods and reference databases, Biopolymers 89 (2008) 392–400, https://doi.org/10.1002/bip.20853.

[53] C. Carter, R.W. Thombur, Germin-like proteins: structure, phylogeny, and function, J. Plant Biol. 42 (1999) 97–108.

[54] A.O. Barel, A.N. Glazer, Spectroscopic studies on papain and some inactive derivatives spectroscopic studies on papain and some inactive derivatives, J. Biol. Chem. 25 (1969) 268–273.

[55] H. Zare, A.A. Moosavi-Movahedi, M. Salami, N. Sheibani, K. Khajeh, M. Habibi-Rezaei, Autolysis control and structural changes of purified ficin from Iranian fig latex with synthetic inhibitors, Int. J. Biol. Macromol. 84 (2016) 464–471, https://doi.org/10.1016/j.ijbiomac.2015.12.009.

[56] A.E. Kabakov, V.L. Gabai, Protein aggregation as primary and characteristic cell reaction to various stresses, Experientia 49 (1993) 706–710, https://doi.org/10.1007/BF01923956.